*34th EPS Conference on Plasma Phys. Warsaw, 2 - 6 July 2007 ECA Vol.**31F**, O-4.018 (2007)*

Core MHD studies in the hybrid regime of JET operation

P.Buratti[1], R.Buttery[2], F.Crisanti[1], E.Giovannozzi[1], T.Hender[2], A.Isayama[3], E.Joffrin[4], P.Smeulders[1], O. Zimmermann[5] and JET-EFDA contributors*

[1]EURATOM-ENEA Fusion Association, C.R. Frascati, CP65, 00044 Frascati, Italy
[2]EURATOM/UKAEA Fusion Association, Culham Science Centre, Abingdon OX14 3DB, UK
[3]Japan Atomic Energy Agency, Naka, Ibaraki 311-0193, Japan
[4]Association EURATOM-CEA, DSM-DRFC, CEN Cadarache, F-13108 St Paul lez Durance, France
[5]Institut für Plasmaphysik, Forschungszentrum Jülich GmbH, EURATOM Association, Jülich, Germany
*See the Appendix of M.L. Watkins *et al.*, Fusion Energy 2006 (Proc. 21st Int. Conf, Chengdu), IAEA, (2006)

The Hybrid regime is an alternative to the ELMy H-mode with absent or very weak sawtooth activity and better prospects of MHD stability at high normalised kinetic pressure (β_N). The main MHD activities observed in the hybrid regime are fishbones, neoclassical tearing modes (NTM), internal kink modes/sawteeth and Alfvén eigenmodes [1]. Plasmas with internal kink modes that saturate at low amplitude have good energy confinement and no impurity peaking [2]. Also discharges with dominant fishbone activity feature good confinement, while the m/n = 3/2 NTM tends to seriously affect confinement. The 2/1 NTM, which restricts beta below the no-wall limit $\beta_N \le 4l_i$ in DIII-D hybrid plasmas [3], was observed at JET in a few cases only, in conjunction with profile modifications provoked by impurity injection or by ELM-free periods, while it was not observed in discharges with $\beta_N / 4l_i$ up to 1.2. The 2/1 NTM is dealt with in [4]. The focus of this paper is on the 3/2 NTM in JET hybrid discharges [5].

Amplitude of the 3/2 NTM

Rotation of a single-m magnetic perturbation produces temperature oscillations with "M-shaped" radial profile (figure 1), whose peak-to-peak distance gives the full island width [6]. In many cases, due either to the presence of a strong 2/2 mode component or to cutoff affecting the ECE diagnostic, this direct information is not available and one has to rely on external magnetic oscillations.

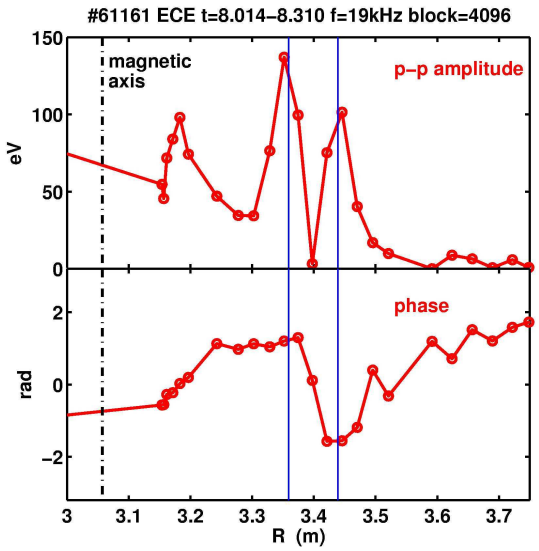

Figure 1. Amplitude and phase of T_e oscillations. Vertical blue lines mark island extremes.

Poloidal field oscillations $\tilde{B}_\theta(b)$ were extracted from the spectrograms of $\dot{B}_\theta$ as the amplitude to frequency ratio of the $n = 2$ line. Radial field at the island was evaluated as

$\tilde{B}_r(r_s) = 0.5(b/r_s)^{m+1}\tilde{B}_\theta(b)$, where coil radius b and resonant radius r_s are referred to the magnetic axis radius R from EFIT equilibrium. The full island width is $w = 4\left(Rr_s\tilde{B}(r_s)/ns_sB_T\right)^{1/2}$ [6], where B_T is toroidal field. Magnetic shear s_s is not well measured; the value s_s = 1, which gives agreement between magnetic and temperature data for the case of figure 1, was chosen once for all. A uniform assumption was also done for r_s, since its measurement from ECE data is not always available: the island major radius was assumed to be $R_s = 3.4$ m for the entire database. As verified on discharges with R_s available from ECE, this assumption introduces errors in w that lie within 20% in most cases, with a few outliers at 40%. Results are shown in figure 2. The island width varies from 1 to 25 cm, clearly increasing with β_N. Besides data points shown in figure 2, the database includes cases (109 out of 279) in which no n = 2 mode is detected and MHD activity is dominated by fishbones.

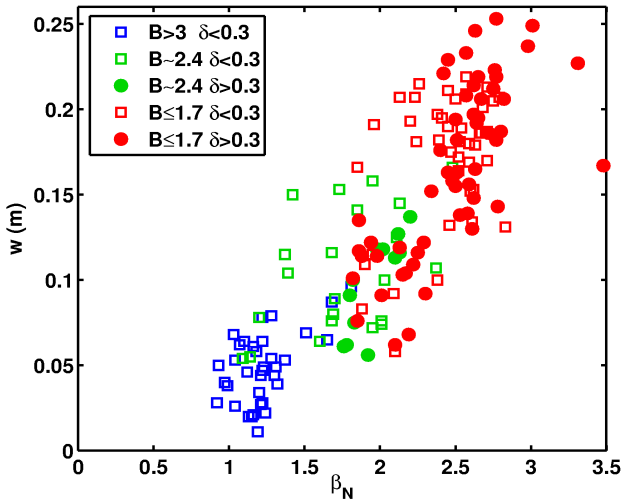

Figure 2. Island width versus normalised beta.

NTMs affect confinement as islands short-circuit radial diffusion. Figure 3 shows discharge that dithers twice between fishbones and NTM-dominated conditions. The $H_{ITER89L-P}$ confinement factor decreases by 10% when the island grows to w = 0.13 m; the relative energy variation is $\delta W/W = 0.6\, w/a$. Analytic estimates based on profile flattening across the island [7] give factors ranging from 0.38 to 1.45, depending on island model and assumed profiles, so JET results are close to the lower bound. Estimated confinement reduction for the biggest observed islands amounts to 20%. Confinement

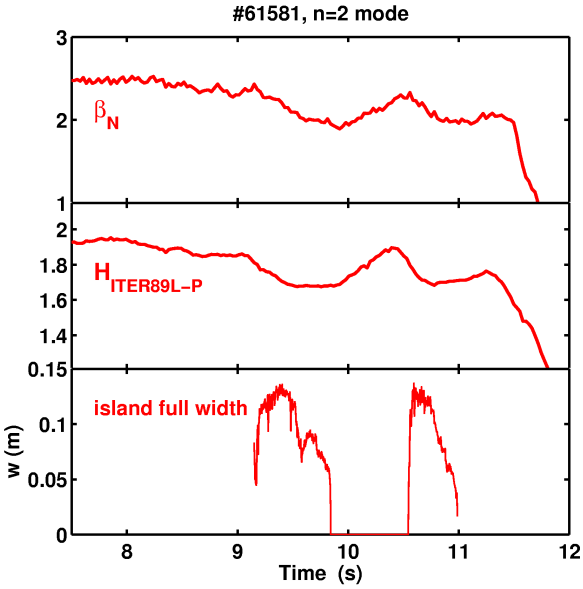

Figure 3. Time history of normalised beta, confinement and island width. Fishbones are present when w = 0.

degradation at the onset of the 3/2 NTM was also observed in ASDEX [8]

Nonlinear NTM stability

For the well-diagnosed case shown in figure 1, the (non-linear) tearing stability index at saturation has been evaluated according to $r_s\Delta'(w) = -4.4(r_s/w)(Rq/B_T s_s)\mu_0 j_{boot}$ [10]. Using R = 3.057 m, r_s = 0.395 , B_T = 2.4 T and the neoclassical bootstrap current $j_{boot} = 1.25\times10^5$ A/m^2 as calculated from TRANSP [9], it turns out $r_s\Delta' = -5.7$, which is very close to the usually assumed lower bound $-2m$. It must be stressed that the observation of spontaneous NTMs indicates that very different values (even positive) occur at smaller w or during current profile evolution.

Observation of spontaneous NTMs

Spontaneous NTMs have been clearly identified; in the example shown in figure 4 an $n = 2$ NTM grows from noise during an ELM-free period lasting from 5.55 s to 5.75 s. The initial island width is smaller than the polarisation threshold [11], while the transport threshold [6] is below the minimum detectable width. The curvature stabilising effect at zero island width [10] is strong, $r_s\Delta'_{GGJ} < -10$ so that the tearing stability index should be positive and large to give classical tearing mode destabilisation; this is difficult to reconcile with the Δ' values estimated at saturation, unless the $\Delta'(w)$ dependence is extremely strong. This problem was pointed out in [12], where triggering by ideal modes was proposed. Tearing modes destabilisation near ideal stability boundaries was considered in [13]; another possibility is that, at least in some conditions, the ion polarisation drift plays a destabilising role.

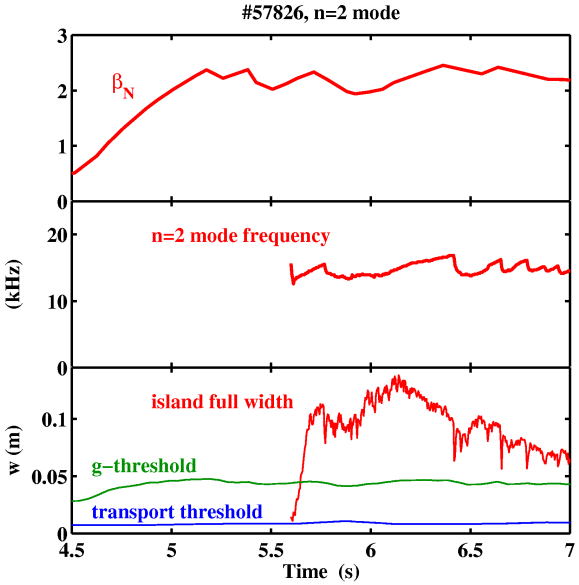

Figure 4. Time history of β_N, NTM frequency and island width showing a spontaneous NTM onset. Transport and ion polarisation (g) thresholds are shown.

NTM frequency

The island rotation velocity generally agrees with plasma velocity as measured by charge exchange diagnostics at the assumed island position R_s = 3.4 m. In addition to this general trend, spectrograms feature two interesting details, namely sidebands and chirping.

Sidebands. NTM lines lie at frequencies between 5 and 30 kHz; in the example shown in figure 5, sidebands with spacing of about 1 kHz appear when the amplitude of magnetic oscillations increases. This indicates the onset of a limit cycle with a period corresponding to the sideband frequency shift, due either to a secondary instability or to interaction between different modes, e.g. with the $n = 3$ mode shown in figure 5. This (presently not identified) modulation mechanism could be a new ingredient to understand NTM saturation.

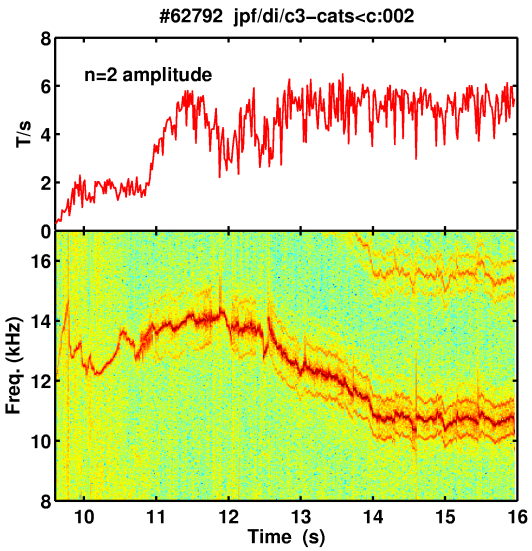

Figure 5. Time history of n=2 mode amplitude and spectrum showing the appearance of sidebands. An n=3 NTM (above 15 kHz) is also shown.

Chirping. At high NBI power the NTM frequency chirps, i.e. it abruptly flips up (by 50% typically) and then recovers in about 1ms. Similar observations were reported in [12]. These frequency variations cannot be due to ELMs or coupling to $m = 1$ modes, since chirping events can be found at times when neither ELMs nor $m = 1$ modes are present. Frequency chirping indicates that a sort of $n = 2$, $m = 3$ fishbone is present. So, in addition to the ordinary bootstrap drive, the mode could tap energy from fast particles.

Conclusions

Neoclassical tearing modes reduce confinement by 20% at high β_N. Frequency spectra point to the existence of new physical mechanisms that can drive/damp NTMs.

References

[1] P. Buratti et al., Plasma Phys. Contr. Fusion **48** (2006) 1005
[2] C. Giroud et al., Nucl. Fusion **47** (2007) 313
[3] T. C. Luce et al., Phys. Plasmas **11** (2004) 2627
[4] R. Buttery et al., paper P1.137 this Conference
[5] E. Joffrin et al., Nucl. Fusion **45** (2005) 626
[6] R.Fitzpatrick, Phys. Plasmas **2** (1995) 825.
[7] Z.Chang, J.D.Callen, Nucl Fusion **30** (1990) 219
[8] J. Stober et al., 21st Fusion Energy Conference, Chengdu 2006, EX/P1-7
[9] R.J.Goldston et al., J. Comp. Physics **43** (1981) 61
[10] H.Lutjens et al., Phys. Plasmas **12** (2005) 080703 and Phys. Plasmas **8** (2001) 4267
[11] R.J.La Haye, O.Sauter, Nucl. Fusion **38** (1998) 987
[12] E. D. Fredrickson, Phys. Plasmas **9** (2002) 548
[13] D.B. Brennan et al., Phys. Plasmas **10** (2003) 1643